Two new species of *Nanofrustulum* (Bacillariophyta) from temporary rivers in the Alentejo region, southern Portugal

Eduardo A. Morales[1,2], Maria Helena Novais[1,2], María Luján García[3]*, Nora I. Maidana[4,5], Maria Manuela Morais[1,2]

[1] Water Laboratory, University of Évora, P.I.T.E. Rua da Barba Rala No. 1, 7005–345 Évora, Portugal

[2] Institute of Earth Sciences – ICT, University of Évora, Rua Romão Ramalho 59, 7000–671 Évora, Portugal

[3] Institut für Geographie, GEOPOLAR, Universität Bremen, Germany

[4] CONICET. Instituto de Biodiversidad y Biología Experimental Aplicada (CONICET – UBA). Buenos Aires, Argentina

[5] Universidad de Buenos Aires. Departamento de Biodiversidad y Biología Experimental (DBBE). Buenos Aires, Argentina

* Corresponding author: garcia@uni-bremen.de

With 35 figures and 2 tables

Abstract: Two new *Nanofrustulum* species, *N. lucectorii* sp. nov. and *N. ibericum* sp. nov. are described from temporary streams in southern Portugal based on light and electron microscopy observations. *Nanofrustulum lucectorii* sp. nov. is characterised by elliptic valves with broadly rounded apices, spines with a solid core, an apically elliptic base, a flattened body, and spatulate, serrate tips that are wider than the spine body. These spines have rectangular stipules covering the first subtending mantle areola. The equal apical pore fields are present at both valve apices and are composed of a single transapical row of sunken pores. *Nanofrustulum ibericum* sp. nov., in turn, is unique in that it has solid spines with a triangular or trapezoid base, and a triangular and recurved body. Additionally, the blisters on the abvalvar side of the mantle are pervalvary rectangular and widely spaced. The morphological features, ecology and distribution of the new species are discussed based on relevant literature.

Key words: biodiversity; morphology; Staurosiraceae; taxonomy; ultrastructure

Introduction

The genus *Nanofrustulum* Round, Hallsteinsen & Paasche (1999) was erected to contain small, roundish to oval diatoms forming chains with the aid of linking spines positioned on vimines at the valve face/mantle region. The striae are composed of areolae containing dissected volae and the girdle is quasifract with fimbriate segments lacking perforations. The typus generis is *N. shiloi* (J.J.Lee, Reimer & McEnery) Round, Hallsteinsen & Paasche (1999: 345, 346), with *Fragilaria shiloi* J.J.Lee, Reimer & McEnery (1980:23) as its basionym, a diatom often reported as an endosymbiont in marine Foraminifera. At the time of description, Round et al. (1999) were unsure of the presence of fully developed apical pore fields in both extremes of the valves of *N. shiloi* stating: "… small apical pore fields or a single pore at one (?) end of the sternum." Li et al. (2018: 47), providing an emended description of the genus, stated that apical pore fields are present in species ascribed to the genus.

Upon morphological observation under scanning electron microscopy (SEM), one of the main distinguishing features of *Nanofrustulum* is the presence of quasifract bands that in our preliminary appreciation vary in size and shape in a species specific manner. However, there is not much information about this feature in species description and characterisation in the literature, thus, conclusions regarding the use of this feature cannot be drawn. Therefore, apical pore fields and quasifract bands remain the most understudied morphological features in species of *Nanofrustulum*.

Medlin & Desdevises (2016) represented *Nanofrustulum* by a single species in the tree, *N. shiloi*, characterised as a marine genus with areolar occlusions, apical pore fields as aggregated small pores, a valve length/width ratio of 1.0–l.2, and the absence of a septum on its girdle bands and absence of labiate processes. None of these characteristics are defining for *Nanofrustulum* as a *bona fide* genus since they might also be present (or absent) in other members of the family Staurosiraceae (type = *Staurosira* (Ehrenberg) Williams & Round [1988]), described in the same work by Medlin & Desdevises (2016), based on the genetic separation of *Nanofrustulum*, *Opephora* Petit, *Plagiostriata* Sato & Medlin, and *Staurosira* as clade 4 from other small and large "araphid" diatoms. As shown by Morales (2001) and Morales et al. (2001), members of *Staurosira*, *Pseudostaurosiropsis* E.Morales, and *Staurosirella* D.M.Williams & Round (the last two genera added to the family without morphological analysis or genetic confirmation in the supertree) meet the exact same morphological criteria used to justify *Nanofrustulum* in the supertree, except for the latter being marine.

Subsequent molecular work also has shown that some of the genera mentioned to be in the Staurosiraceae do fall together in the same clade (e.g. Theriot et al. 2010, Ashworth et al. 2012) but a clear justification for this grouping and the relationships within it at the genus level remain elusive, as stated by Li et al. (2018). These latter authors, supported also by Morales et al. (2019), find that this lack of resolution in the staurosiroid (term as used by Theriot et al. 2010) diatoms is due to the lack of a wider taxon sampling within the group. Morales et al. (2019, 2021) add that there is a lack of treatment of molecular and morphological information using a common methodology to produce more robust

analyses and phylogenies (e.g. as done by Frankovich et al. 2018), and that molecular results thus treated could become a firmer basis for the recognition of features that are evidence for relationships among the groups (see Cox 2010). This debate is not new, as it has been going on for decades and it still remains an open discussion to find congruences between molecular phylogenies and morphology (Patterson et al. 1993, Williams 2006, Williams 2013).

Morales et al. (2019), in an effort to find distinguishing morphological features for small "araphid" genera lacking a rimoportula, established that the girdle element structure could be used to characterise *Nanofrustulum* as a separate genus since its species have open copulae of the quasifract type with developed fimbriae. Within the Staurosiraceae, which also includes *Punctastriata* D.M.Williams & Round, *Sarcophagodes* E.Morales, *Stauroforma* Flower, V.J.Jones & Round and *Trachysphenia* Petit (again, placed in this family without genetic confirmation in the Medlin & Desdevises (2016) supertree), the quasifract copulae of *Nanofrustulum* are unique to this genus.

Besides the habit of the generitype (*N. shiloi*) as endosymbiont, species of *Nanofrustulum* have also been reported from marine benthic habitats, especially sediment samples from the intertidal and subtidal zones (e.g. Witkowski et al. 2010, Li et al. 2018), and from the nanoplankton (Sar & Sunesen 2003, Li et al. 2008). They apparently are relatively easy to culture, as well (López-Fuerte et al. 2016), which has favored their use as experimental organisms (e.g. Li et al. 2018, Demirel et al. 2020, Glaviano et al. 2021). Other reports of *Nanofrustulum* come from brackish and freshwater habitats, where samples were collected mainly from epilithic and depositional habitats (mud, sand, and sediment cores) from lakes and rivers, and even waterfalls (e.g. Wetzel et al. 2013, Grana et al. 2015). Ruocco et al. (2018, 2020) collected *N. shiloi* as an epiphyte growing on *Posidonia oceanica* (Linnaeus) Delile from the coast of Italy and Glezer et al. (1992) collected *N. cataractarum* (Hustedt) C.E.Wetzel, E.Morales & Ector from wet moss in hot springs of the Kamchatka region, Russia.

In the present work we describe two new species of *Nanofrustulum* from temporary rivers in southern Portugal, collected as epilithic taxa, the first observations for this type of ecosystems. The ecology of the new taxa as well as their morphological features is contrasted with all species currently ascribed to the genus.

Materials and Methods

Diatoms were collected in 2017 from several temporary streams in southern Portugal. A complete list of these streams, as well as their ecological characteristics, can be found in Novais et al. (2020). The localities where the two new taxa were observed are included in Table 1 and Fig. 1. Simultaneously to diatom sampling, a thorough hydromorphological characterization of a 500 m stretch of each stream (upstream of the sampling point, whenever possible) was carried out, following the River Habitat Survey Methodology (INAG I.P. 2008), including information on the substrate type of vegetation present in the

Table 1. Localities (streams) in southern Portugal where *Nanofrustulum lucectorii* sp. nov. and *N. ibericum* sp. nov. were found.

Stream name (as in Fig.1)	Geographical location	Date of collection (2017)	Type of sample	Relative abundance (%)	
				N. lucectorii sp. nov	*N. ibericum* sp. nov.
Amieira	38°16'51,78" N, 7°36'21,62" W	Sept. 22	Pool	0	2.8
		Sept. 22	Dry biofilm	7.6	0
Cuncos	38°25'28,47" N, 7°17'23,66" W	Oct. 11	Dry biofilm	1.4	0
Freixial	37°41'15,52" N, 7°39'46,19" W	May 19	Pool	31.1	0
		Sept. 20	Dry biofilm	4.2	0.5
João Dias	37°51'17,75" N, 7°18'00,52" W	May 26	Stream	1.3	0
		Sept. 21	Stream	1.4	0
Lampreia	37°32'59,19" N, 7°43'41,09" W	Mar. 29	Stream	1.2	0
		Sept. 19	Pool	2	0
		Sept. 19	Dry biofilm	20.6	0
Limas	37°49'19,91" N, 7°37'21,18" W	Apr. 21	Stream	2.4	0
		Sept. 20	Pool (type sample)	17.4	8.4
		Sept. 20	Pool	17.5	2.1
		Sept. 20	Dry biofilm	37.0	6.8
Maria Delgada	37°39'36,42" N, 8°05'43,35" W	Mar. 29	Stream	0.4	1.7
		Sept. 19	Pool (type sample)	11.9	25.9
		Sept. 19	Dry biofilm	29.8	40.4
Oeiras	37°32'51,45" N, 7°59'45,01" W	Mar. 29	Stream	7.2	0
		Sept. 29	Pool	40.6	0
		Sept. 29	Dry biofilm	31.4	1.7
Palheta	38°39'45,50" N, 7°41'40,08" W	Oct. 11	Dry biofilm	0.6	0
Porteira Rija	38°11'41,92" N, 8°09'26,92" W	Apr. 7	Stream	0.9	0.4
		Sept. 28	Dry biofilm	24.7	0

Fig. 1. Location of the sites where *Nanofrustulum lucectorii* sp. nov. ("x", black star indicates the type locality), and *N. ibericum* sp. nov. (open circles, black circle indicates the type locality) were found.

channel, flow types, land-use within 5 and 50 m of the left and right banktops, vegetation structure in banktops and bank-faces, bank profiles, height of banktop, and other dimensions such as the height above the water surface, channel (bankfull and water) width and depth, and presence of special features, as well as nuisance species and alders. Water chemistry was determined *in situ* using the TROLL 9500 PROFILER XP (In-Situ Inc. Fort Collins, Colorado, U.S.A.), at the time the biological samples were collected. Nutrient data were determined in the laboratory using the methodology outlined in Novais et al. (2020). Biological samples were collected from rocks under flowing water, in pools, and from exposed rocks covered in dry biofilm, following the methodology outlined in Novais et al. (2020). Five to seven hand-sized rocks were selected randomly, and scrubbed with a toothbrush, rinsed with stream water, and preserved with formaldehyde (1:1 v/v) right after collection. Aliquots from each sample were oxidized in the laboratory with hydrogen peroxide (35%) in a sand bath (210 °C) for 36 h after which the material was rinsed with distilled water until neutrality (INAG I.P. 2008). Permanent slides were mounted in Naphrax and diatom valves were identified to species level using a Leica DMLB light microscope equipped with a ×100 HCX PL APO oil immersion objective (N.A. 1.40) and a Leica DC 500 camera. A minimum of 400 valves was identified and counted on each slide in order to assess the relative abundance of taxa composing the community (INAG I.P. 2008). The identification was based on reference floras (e.g. Krammer & Lange-Bertalot 1986, Krammer & Lange-Bertalot 1988, Krammer & Lange-

Bertalot 1991a, Krammer & Lange-Bertalot 1991b, Hofmann et al. 2011, Lange-Bertalot et al. 2017) as well as recent bibliographic sources, including the series "Diatoms of Europe", "Iconographia Diatomologica", "Bibliotheca Diatomologica" and relevant taxonomic papers, such as Reichardt (1997), Van de Vijver et al. (2011) and Novais et al. (2011).

For SEM observations, material in suitable conditions (less organic material, higher number of entire valves and reasonably high abundance of the studied taxa) were selected. For this, aliquots of the cleaned material were dried on aluminum stubs at room temperature before being coated with gold (20 nm thickness) and examined using a Carl Zeiss SUPRA 40 (15 kV) at the Centro de Microscopías Avanzadas (CMA), FCEN, Universidad de Buenos Aires, Argentina.

Morphological terminology follows Anonymous (1975, stria, areola and spine morphology), Ross et al. (1979, stria, areola and spine morphology), Barber & Haworth (1981, valve shape and striation pattern), Williams & Round (1988, areolar substructures, apical pore fields, and girdle band features), and Round et al. (1990, areolar substructures, apical pore fields, and girdle band features).

The Specific Pollution Sensitivity Index (SPI) was calculated from diatom abundances (Coste in Cemagref 1982), using the OMNIDIA v. 5.5 software (Lecointe et al. 1993). Additionally, the Ecological Quality Ratio (EQR) was calculated based on recommendations of APA, I.P. (2016). River typology corresponds to that presented in INAG I.P. (2008).

Results

Nanofrustulum lucectorii **E.Morales, Novais, M.L.García & Maidana sp. nov.**

Description: Frustules rectangular in girdle view (Fig. 12). Valves elliptic with broadly rounded apices (Figs 2–11); length 4–14 µm, width 3.5–4.0 µm, stria density 14–15 in 10 µm. Sternum narrowly lanceolate, externally below virgae, internally below virgae but above striae (Figs 2–14, 24, 26). Virgae doubly flared, externally and internally raised (Figs 24–26). Valve face/mantle transition somewhat gradual, as thick valve contour (Figs 2–11). Valve mantle edge parallel to valve face-mantle junction, except at apices where mantle slightly curved in pervalvar (Figs 24, 26, 29). Striae parallel at valve center, radiate toward valve apices, composed of large, round to transapically or pervalvary trapezoid areolae (Figs 24–29), 3–4 per 10 µm. Striae at same level as axial area externally, internally sunken in depressions below axial area and virgae (Figs 24–26). Branched volae transapically arising from inner areolar periphery (Figs 27, 28). One to four areolae on valve face decreasing in size from valve face/mantle transition. One to two, occasionally four areolae on mantle, decreasing in size advalvary. Flaps produced on valve mantle (Figs 27, 29). Spines located on vimines, arising from a single point and stopping shortly before valve apices; apically elliptic base, flattened body with solid core, spatulate, serrate tips wider than spine body; large (Figs 24, 25, 27–29), rectangular stipules present
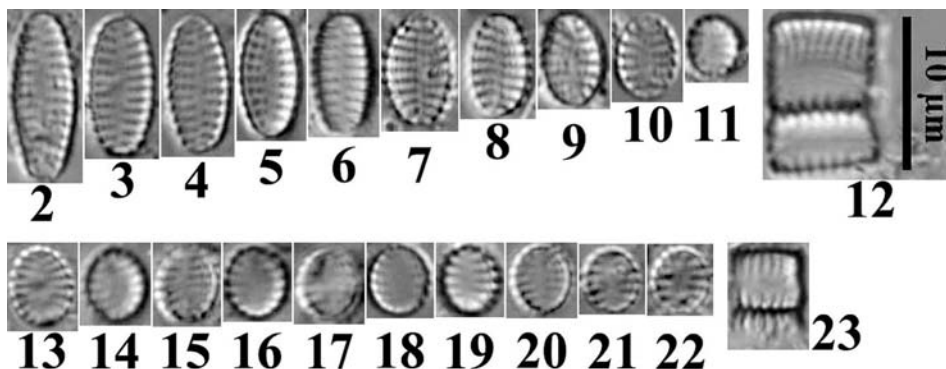
Figs 2–23. LM images of new *Nanofrustulum* species from temporary rivers in southern Portugal. 2–12. Size diminution series for *N. lucectorii* sp. nov. from Limas stream, Portugal, the type locality (BR-4783). Fig. 3 corresponds to the holotype specimen. Fig. 12 shows two cells attached in girdle view. 13–23. *Nanofrustulum ibericum* sp. nov. from Maria Delgada stream, Portugal, the type locality (BR-4784). Fig. 18 corresponds to the holotype specimen. Fig. 23 shows the girdle view of an entire frustule and a neighboring valve still attached. Scale bar = 10 μm.

extending above first subtending mantle areola (Figs 28, 29, white arrowheads). Apical pore fields externally cavernous sunk, of similar size in both valve apices, with single row of sunken pores (Figs 24, 25, white arrows). Internally, single row of small, round pore openings within an elliptic depression (Fig. 26, white arrows). Cingulum composed of open, unperforated valvocopula (Fig. 29, white asterisk), with numerous copulae progressively and advalvary reduced in size (Fig. 29, black arrows).

Etymology: The specific epithet *ectorii* honors our dear and late colleague and friend Luc Ector. A myriad were the moments and the information exchanged with him over years of close friendship and fluent scientific collaboration. His indefatigable endeavors with the diatoms were an example to many of us.

Holotype: Slide BR-4783 (holotype specimen Fig. 3, LM), Botanical Garden Meise, Belgium. Population partially depicted here in Figs 2–12 (LM) and Figs 24–29 (SEM).

Type locality: Portugal: Limas stream (37°49'19.91" N, 7°37'21.18" W), Municipality of Serpa, southern Portugal, leg. E. Morales & J. Figueira, coll. date 20.IX.2017.

Habitat: Epilithic in temporary rivers with low water depth. Also collected from dry biofilms on rocks but unclear whether cells were alive or not.

Ecology and distribution: The Limas stream is a temporary river that dries out to isolated pools at the end of the summer and is classified within the "Rivers from the south of medium-large dimensions", according to the Water Framework Directive typology. The stream is located in a deep V-shaped valley without natural terraces or a distinct flat valley bottom. Water is not impounded by a dam, but the site is interrupted by a bridge with several culverts (15 for a 50 m width of channel from bank to bank). The bed material is
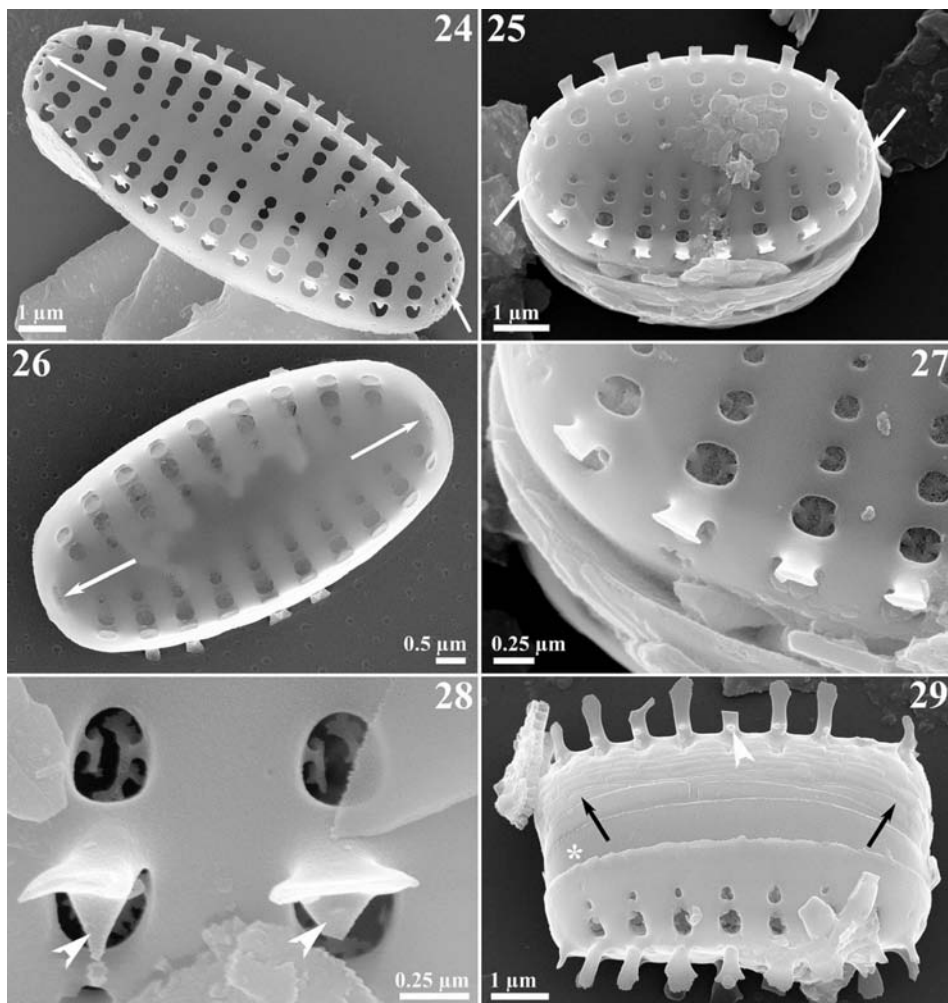
Figs 24–29. SEM images of *Nanofrustulum lucectorii* sp. nov. 24. External view of partially eroded valve showing pattern of areolation, linear to lanceolate sternum, position of spines, and features of apical pore fields (white arrows) (Limas stream, type locality). 25. External view showing previous features and confirming position of the rugged apical pore fields on the advalvar region of the apical mantle (white arrows) (Maria Delgada stream). 26. Internal view showing shallow depressions into which the areolae open internally. White arrows indicate the internal depression into which the apical pores open (Oeiras stream). 27. Close up of Fig. 25. Dichotomously branching volae can be seen, arising transapically from the inner border of each areola. Spines interrupt the striae at the valve face/mantle junction. 28. Close up of a section of the valve face/mantle junction. Notice volae in the areolae, the flat, apically expanded spines and triangular remains of the stipules (white arrowheads) (Maria Delgada stream). 29. Entire frustule in girdle view. Notice wide valvocopula (white asterisk) and progressively fragmented (quasifract) copulae (black arrows). Serrate spines can also be seen on the upper left part of the image (Maria Delgada stream).

of siliceous lithology, unconsolidated with large boulders present. The vegetation was characterized by emergent broad-leaved herbs, emergent reeds, sedges, rushes, grasses, horsetails, and filamentous algae. The land-use within 5–50 m of the banktops includes a hill with a semi-natural broadleaf/mixed woodland and rough unimproved grassland/pasture, with cattle sporadically present. While the other side is dominated by a paved road and scrub and shrubs. At the time of sampling, the dry river bed was about 60%, while the wet part was 40%, with large pools with standing water. Two of these pools were sampled, one of them was $> 100 \times 30$ m in size and > 1 m deep, while the other was 5×2 m and 30 cm deep. The large pool was about 15% shaded by trees and had a bottom dominated by sand and gravel mixed with larger rocks, while the smaller one was not shaded and had cobbles and gravel mixed with larger rocks. The species was also found on dry biofilm that was sampled from rocks outside these pools.

At the time of sampling, water temperature of the larger pool was 27.6 °C and 33.8 °C for the smaller pool (at 11:40 AM–13:22 PM), turbidity 13.0 and 7.6 NTU, pH 8.7 and 8.8, electrical conductivity 946.0 and 742.5 μS·cm^{-1}, dissolved oxygen 68.5 and 79.8% sat., phosphates 0.06 and 0.17 mg·L^{-1} PO$_4$, nitrates 2.68 and 1.92 mg·L^{-1} NO$_3$, respectively. Though the dry biofilm had a larger relative abundance of the new taxon (37.0%), due to the suitable quality of material for SEM analysis, the first, larger pool was chosen as the source of the type material, which contained a relative abundance of 17.4%. The second smaller pool also contained a similar relative abundance of 17.5%.

At this site (based on the diatom flora found in the first pool), the stream was classified as Good (SPI = 12.4, EQR = 0.76 since the reference value for this typology is 16.35), according to the class boundaries depicted in APA (2016) for the Biological Quality Element Phytobenthos-diatoms.

This new taxon was found in 8 other localities (Fig. 1, Table 1), varying in relative abundance from 0.4% (in rocks from flowing waters of Maria Delgada stream) to 40.6% (in rocks from a pool in Oeiras stream).

Associated flora: At the type locality the taxon shared habitat with *Amphora pediculus* (Kützing) Grunow (9.6% relative abundance), *Pseudostaurosira* sp. 2 (9.0%, a small roundish form), *Nanofrustulum ibericum* sp. nov. (8.4%, see below), *Karayevia clevei* (Grunow) Bukhtiyarova (8.0%), *Pseudostaurosiropsis* sp. 2 (8.0%, a form smaller than *Pseudostaurosira brevistriata* (Grunow) D.M.Williams & Round), and *Epithemia adnata* (Kützing) Brébisson (5%).

Nanofrustulum ibericum E.Morales, Novais, M.L.García & Morais sp. nov.

Description: Frustules rectangular in girdle view (Fig. 23). Valves broadly elliptic with broadly rounded apices (Figs 13–22), sometimes with a flat face; length 4.5–5.5 µm, width 3.5–4.0 µm, stria density 20–30 in 10 µm. Sternum lanceolate to broadly lanceolate, externally below virgae, internally below virgae but above striae (Figs 30–32, 35). Virgae doubly flared, though flaring at valve face unnoticeable due to very small areolae; slightly raised externally, internally raised (Figs 30–32). Transition between valve face and valve mantle abrupt (Figs 30, 33). Valve mantle edge convex, becoming conspicuously
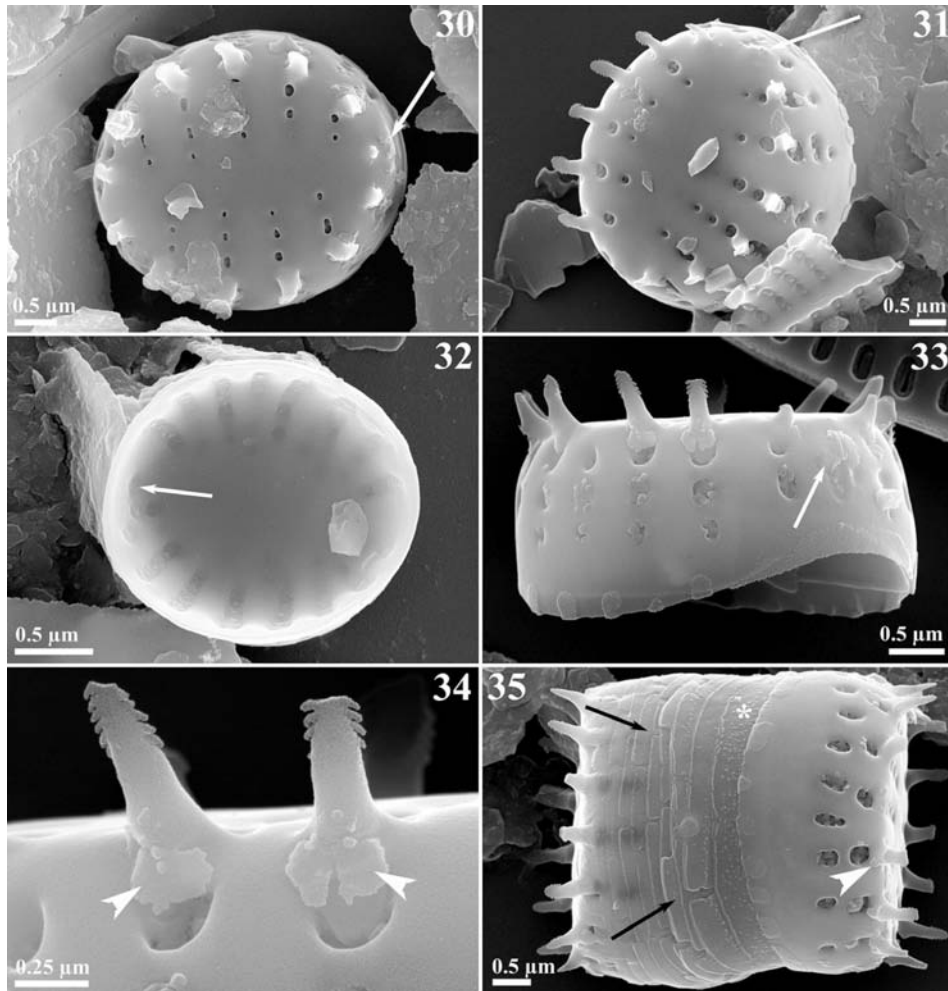
Figs 30–35. SEM images of *Nanofrustulum ibericum* sp. nov. 30. External view showing pattern of areolation, features and location of spines, wide sternum and apical pore field located on one apex (white arrow) (Limas stream). 31. External view showing previous features and the unique rugged apical pore field (white arrow). Transapically arising volae can be seen tightly packed within each areola (Maria Delgada stream, type locality). 32. Internal view showing shallow depressions into which the areolae open internally. White arrow indicates internal depression into which the apical pore field opens (Limas stream). 33. Side view of a valve showing deep pattern or areolation on mantle, serrated spines, flaps and the rugged, occluded apical pore field (white arrow) (Maria Delgada stream, type locality). 34. Close up of Fig. 33 focusing on serrated spines and subtending flap-like stipules (white arrowheads). 35. Entire frustule in side view showing quasifract valvocopula (white asterisk) and copulae (black arrows). Also notice the flap-like stipule (white arrowhead) subtending the serrate spines (Maria Delgada stream, type locality).

curved in pervalvar sense at the valve apices (Figs 33, 35). Siliceous plaques along abvalvar valve mantle edge (Figs 33, 35). Striae parallel, radiate toward valve apices, composed of round to transapically or pervalvary elongate areolae (Figs 13–22, 30, 31, 33, 35). Striae at same level as axial area externally, internally sunken in depressions below axial area and virgae (Figs 30–33, 35). Branched volae arise transapically from the inner areolar periphery (Figs 31, 35). 2–3 areolae on valve face, decreasing in size from valve face/mantle transition. 2–3 large areola on valve mantle, decreasing, increasing, or increasing and decreasing in size again advalvary (Figs 30, 31, 33, 35). Flaps produced on valve mantle (Fig. 33). Spines located on vimines, arising from a single point, stopping before or continuous around valve apices (Figs 30, 31), triangular to transapically trapezoid base with a solid core, triangular, recurved body, spatulate, serrate, tapering tips (Figs 30, 31, 33–35). Flap-like stipules partially covering first subtending mantle areola (Figs 34, 35, white arrowheads). Apical pore fields externally with 2–3 poroids located on one extreme of the valve, covered by flaps (Figs 30, 31, 33, white arrows). Internally pores indistinguishable (occluded). Internal apical depression (Fig. 32, white arrow). Cingulum composed of quasifract unperforated valvocopula (Fig. 35, white asterisk), copulae progressively and advalvary reduced in size (Fig. 29, black arrows).

Etymology: "*ibericum*" refers to the Iberian Peninsula, the first place from which the new taxon is reported herein.

Holotype: Slide BR-4784 (holotype specimen Fig. 18, LM), Botanical Garden Meise, Belgium. Population partially depicted here in Figs 13–23 (LM) and Figs 30–35 (SEM).

Type locality: Portugal: Maria Delgada stream (37°39'36.42" N, 8°5'43.35" W), Municipality of Castro Verde, southern Portugal, leg. M. Morais, E. Morales & J. Figueira, coll. date 19.IX.2017.

Habitat: Epilithic in temporary rivers with low water depth.

Ecology and distribution: The Maria Delgada stream is a temporary river that also dries out to isolated pools at the end of the summer and is classified within the "Rivers from the south of small dimensions", according to the Water Framework Directive typology. The stream is located in a concave bowl a distinct flat valley bottom and without natural terraces. The bed material is unconsolidated and composed of bedrock, boulders, grabble, pebbles, cobbles, and silt. The vegetation was characterized by emergent broad-leaved herbs, emergent reeds, sedges, rushes, grasses, horsetails, submerged broad-leaved, submerged linear-leaved, submerged fine-leaved plants, and filamentous algae. The land-use within 5–50 m of the banktops include a rippled terrain with a broadleaf/mixed plantation, scrub and shrubs, and a tall herb/rank vegetation. At the time of sampling, the dry river bed was about 75% of the channel area, while the wet part was 25%, with a single pool with standing water. This pool was 28.2×9.7 m in size and 50 cm deep, with no shading. Dry biofilm was also collected from this locality and contained the highest relative abundance of the new taxon (40.4%) but due to the quality of the material for SEM analysis and the availability of water chemistry data for the pool, the latter was chosen as the type sample and contained 25.9% relative abundance of the new taxon.

Table 2. Salient morphological features of the known species of *Nanofrustulum* including the two new species described herein. Characters that distinguish at species-level in bold.

Feature/ Taxon	*N. cataractarum*	*N. ibericum* sp. nov	*N. krumbeinii*	*N. lucectorii* sp. nov.	*N. neoellipticum*
Habitat and shape	Freshwater	Freshwater	Marine	Freshwater	Freshwater
Dimension in µm	L: 5.8–8.2 W: 5.4–7.2 L/W: 1.1	L: 4.3–5.4 W: 3.5–3.9 L/W: 1.2–1.4	L: 1.5–4.5 W: 1.5–4.5 L/W: 1	L: 4.1–11.3 W: 3.6–4.1 L/W: 1.1–2.8	L: 3–14 W: 2–4 L/W: 1.5–3.5
Stria density in 10 µm	15–18	20–30	18–25	14–15	12–15
Areola density in 1 µm	3	4.0–4.2	4	3–4	1.4–4
Valve shape	Round to broadly elliptic with broadly rounded apices	Broadly elliptic with broadly rounded apices	Broadly elliptic to broadly ovate with broadly rounded to obtuse apices	Elliptic with broadly rounded apices	Narrowly elliptic with cuneate or broadly rounded apices
Sternum	Broadly elliptic to rounded	Lanceolate to broadly lanceolate	Irregularly linear	Narrowly lanceolate	Narrowly lanceolate to lanceolate
Striae/ areolae/ volae/flaps	Radiate throughout, composed of small, round to transapically or pervalvary elongate areolae. Profusely branched volae arise from the deep inner contour of each areola. 1–4 areolae on valve face barely decreasing in size from valve face/ mantle transition. 1-5 areolae on valve mantle, barely decreasing in size advalvary. Flaps absent	Parallel to radiate toward valve apices, composed of round to transapically or pervalvary elongate areolae. Branched volae arise apically from the inner areolar periphery. 2–3 areolae on valve face, decreasing in size from valve face/ mantle transition. 2–3 large areola on valve mantle, decreasing, increasing, or increasing and decreasing in size again advalvary. Flaps produced only on valve mantle	Parallel to slightly radiate toward valve apices, composed of round to apically elongate areola on valve face, pervalvary trapezoid on valve mantle. Profusely branched volae arise transapically from the inner areolar contour on valve face, apically on valve mantle. 1–4 areolae on valve mantle, decreasing in size from valve face/mantle transition. 2–3 areolae on valve mantle decreasing in size advalvary. Sometimes, contiguous areola fuse to form a single apically elongate areola (vimines are not produced). Flaps absent	Parallel to radiate toward valve apices, composed of large, round to transapically or pervalvary trapezoid areolae. Branched volae arise apically from the inner areolar periphery. 1–4 areolae on valve face decreasing in size from valve face/ mantle transition. 1–2 (uncommonly 4) areolae on mantle, decreasing in size advalvary. Flaps produced only on valve mantle	Parallel to radiate toward valve apices, composed of small, round, squarish and transapically or pervalvary trapezoid areolae. Branched volae arise from the deep inner areolar contour. 1–3 areola on valve face and mantle, decreasing in size from the valve face/mantle transition. Flaps absent
Sternum/ striae/virgae complex	Externally, valve face flat or virgae slightly raised above sternum and striae in smaller specimens. Internally, sternum and virgae raised at same level, striae sunken	Externally, virgae slightly raised, sternum and striae sunken at same level. Internally, three levels with virgae raised above, sternum in the middle and striae at bottom	Externally, three levels with virgae raised above, sternum in the middle and striae at bottom. Internally, sternum and virgae raised at same level, striae sunken	Externally, virgae raised, sternum and striae sunken at same level. Internally, three levels with virgae raised above, sternum in the middle and striae at bottom	Externally and internally, sternum and virgae raised at same level, striae sunken, the latter more conspicuously in internal view
Blisters on abvalvar side of mantle	Large and irregular	Pervalvary rectangular, widely spaced	Elliptic	Absent	Elliptic to rectangular

N. rarissimum	*N. shiloi*	*N. sopotensis*	*N. sourniae*	*N. squammatum*	*N. trainorii*
Freshwater	Marine	Fresh and brackish	Marine	Marine	Fresh and brackish water
L: 7.3–9.5 W: 2.5–3.3 L/W: 2.9	L: 2–6 W: 2–5 L/W: 1–1.2	L: 3–6 W: 3–4 L/W: 1–1.5	L: 2–12 W: 2.0–3.5 L/W: 1–3.4	L: 2.1–3.3 W: 1.6–2.3 L/W: 1.3–1.4	L: 1.9–8.6 W: 1.7–4.4 L/W: 1.1–2.0
13–14	15	13–17	16–30	35–40	(15) 20–25 (30)
4.2–5.2	2	4	1.2–4.0	1.2–4	3.5
Ovate with rounded head pole and narrowly rounded to broadly rostrate foot pole	Round with broadly rounded apices	Broadly elliptic with broadly rounded to obtuse apices	Round to ovate with broadly rounded or rounded head pole to broadly rostrate foot pole	Broadly elliptic with broadly rounded to obtuse apices	Round to broadly elliptic with broadly rounded to obtuse apices
Linear	Linear to narrowly lanceolate	Linear to narrowly lanceolate	Linear	Linear to irregularly lanceolate	Linear
Biseriate, parallel to radiate toward valve apices, composed of round, square, or apically, transapically or pervalvary trapezoid and elliptic areolae. Branched volae arise transapically on valve face and pervalvary on mantle from inner areolar contour. 1–3 rows of areolae per stria, with variable size reduction. Sometimes, contiguous areola fuse to form a single apically elongate areola (viminules are not produced). Flaps absent	Parallel to radiate toward valve apices, composed of round, transapically or pervalvary elliptic areolae. Profusely branched volae arise apically from inner areolae periphery. 1–4 areolae on valve face and mantle with variable size reduction. Upright flap-like growths arise from areolar border giving the impression of a spiny valve face	Parallel to radiate toward valve apices, composed of round to apically elliptic areolae on valve face, squarish to pervalvary or apically elliptic on mantle. Branched volae arise apically from valve inner periphery in valve face areolae, for entire inner contour in mantle areolae. 1–6 areolae on valve face, decreasing in size from valve face/ mantle transition. 1–3 areolae on mantle decreasing in size adlavary. Flaps produced only on valve mantle	Parallel to slightly radiate toward valve apices, composed of large, round, transapically elliptic or square areolae. Profusely branched volae arise from areolar inner periphery. 1–2 areolae per striae on valve face and mantle, decreasing in size from valve face/mantle transition. Flaps absent	Parallel to radiate toward valve apices, composed of round, transapically or pervalvary rectangular areolae. Branched volae arise from the inner areolar periphery. 1–5 areolae on valve face, only slightly decreasing in size from valve face/mantle transition. 1-3 areolae on valve mantle, adlavary decreasing in size. Flaps absent	Parallel to radiate toward valve apices, composed of round, transapically and pervalvary elliptical or rectangular areolae. Profusely branched volae arising apically from inner areolar contour. 1–6 areolae on valve mantle, decreasing in size from valve face/mantle junction. 1–5 areolae on valve mantle pervalvary decreasing in size. Flaps produced only on valve mantle
Externally, virgae raised, sternum and striae sunken at same level. Internally, sternum and virgae raised at same level, striae sunken	Externally, valve face flat or striae slightly sunken below sternum and virgae. Internally, sternum and virgae raised at same level, striae sunken	Externally, virgae raised, sternum and striae sunken at same level. Internally, three levels with virgae raised above, sternum in the middle and striae at bottom	Externally, virgae raised, sternum and striae at same level. Internally, sternum and virgae raised at same level, striae sunken	Externally and internally, sternum and virgae raised at same level, striae sunken	Externally, virgae raised, sternum and striae at same level. Internally, sternum and virgae raised at same level, striae sunken
Irregular	Irregular	Thin and elongate, widely spaced	Irregular alternating with large depositions, widely spaced	Absent	Rectangular

Table 2. cont.

Feature/ Taxon	*N. cataractarum*	*N. ibericum* sp. nov	*N. krumbeinii*	*N. lucectorii* sp. nov.	*N. neoellipticum*
Spines	Located on vimines or virgae, arising from a single point and continuous around valve apices. Apically elongate to round base and body, the latter with solid core and concave external side, and flattened, serrate tips, slightly slender than spine body. Stipules absent	Located on vimines, arising from a single point and stopping before or continuous around valve apices. Triangular to transapically trapezoid base with solid core, triangular, recurved body, spatulate, serrate, tapering tips. Flap-like stipules partially covering subtending first mantle areola	Located on vimines, arising from a single point and stopping shortly before valve apices. Square to shapeless base, cuboid body with solid core, spatulate, tapering tips. Stipules absent	Located on vimines, arising from a single point and stopping shortly before valve apices. Apically elliptic base, flattened body with solid core, spatulate, serrate tips wider than spine body. Large, rectangular stipules present extending above first subtending mantle areola	Located on vimines, arising from a single point and stopping before valve apices. Circular to apically elliptic base, cylindrical body with soft core, spatulate tips slightly wider. Stipules absent
Apical pore fields	Absent	Externally, 2–3 poroids located on one extreme of the valve are covered by flaps. Internally pores are indistinguishable (occluded) and there is an internal apical depression	Externally, 2-4 round poroids, arranged in at least 2 rows, are located on one extreme of the valve. Internally, round pores open into an elliptic depression	Externally, cavernous and sunken and of similar size in both valve apices, with a single row of sunken pores. Internally, a single row of small, round pore openings lie within an elliptic depression	Externally, semicavernous, large and sunken into both valve apices. One of the pore fields seems to be larger than the other, though difficult to appreciate. Composed of 3 (rarely 4) rows of sunken round poroids. Internally round pores open into an elliptic depression
Reference	Wetzel et al. (2013), Beauger et al. (2018)	This manuscript	Lange-Bertalot & Genkal (1999)	This manuscript	Morales (2021)

At the time of sampling, water temperature in the pool was 15 °C (at 8:45–11:10 AM), turbidity 45.7 NTU, pH 9.0, electrical conductivity 2280.0 $\mu S \cdot cm^{-1}$, dissolved oxygen 45.7% sat., phosphates 0.08 $mg \cdot L^{-1}$ PO_4, and nitrates 9.38 $mg \cdot L^{-1}$ NO_3.

At this site, the stream was classified as Good (SPI = 10.6, EQR = 0.65 since the reference value for this typology is 16.35) (APA 2016).

This new taxon appeared in 5 localities (Fig. 1, Table 1), varying in relative abundance from 0.5% (in dry biofilm in Freixial stream) to 40.4% (in dry biofilm in Maria Delgada stream). The new taxon did not always coexist with *N. lucectorii* but they were found sympatrically in several samples collected from rocks in flowing waters, from pools or more commonly from dry biofilm.

In general, *N. lucectorii* had higher abundance records (> 10%) than *N. ibericum*. In fact, the former species had 10 of these higher records, 5 from epilithon in pools and 5 in dry biofilm, though in the latter samples *N. lucectorii* attained higher abundance ranging from 20.6 to 37.0%.

N. rarissimum	N. shiloi	N. sopotensis	N. sourniae	N. squammatum	N. trainorii
Located on vimines, arising from two points and stopping before valve apices. Apically elongate base, conical body with lateral extensions folded onto the main spine solid body, pointy tips. Stipules absent	Located on vimines, arising from a single point and continuous around valve apices. Triangular base with solid core, cylindrical, twisted body with growths on inner side; spatulate, serrate tips of variable width. Long, W- or V-shaped stipules partially covering subtending first mantle areola	Located on vimines, arising from a single point and stopping before valve apices. Triangular base with solid core, flattened body, spatulate, serrate tips, wider than spine body. Flap-like stipules partially covering subtending first mantle areola	Located on vimines, arising from a single point and stopping before valve apices. Round base, conical body with solid core, spatulate, serrate tips, slightly wider than spine body. Stipules absent	Located on vimines, arising from a single point and continuous around valve apex without an apical pore field. Round base, conical body with solid core, tapering tips with very small lateral projections (serrate). Stipules absent	Located on vimines, arising from a single point and stopping shortly before valve apices. Triangular base with solid core, flattened body, spatulate, serrate tips same width as spine body. Flap-like stipules partially covering subtending first mantle areola
Externally, cavernous, covered by extra siliceous material, with round pores well-sunken and arranged in 2–3 rows. Head pole field much more reduced than foot pole one. Internally, both fields of round pores open into apical depressions	Externally, a single round, sometimes rimmed pore opens at the valve surface. Internally the round opening surfaces into a small roundish depression	Externally, 2–3 round pores are covered by flaps. Fields of both valve apices seem to be unevenly developed, but this is hardly distinguishable. Internally, the pore openings cannot be discerned (occluded)	Externally, cavernous, with uneven round pores, arranged into 1–3 rows, sunken into the valve apex. Can be absent in smaller specimens, but in larger ones, field at foot pole is much larger. Internally, round pore openings lie within shallow depressions	Externally, cavernous, with round, well-sunken pores, arranged in 1–4 rows. Fields of both valve apices are unevenly developed, sometimes absent from one apex. Internally, small, round pore openings of larger fields lie within an elliptic depression; pores of smaller fields surface directly into internal valve face	Absent or reduced to 2–3 round poroids located on one extreme of the valve and sometimes covered by flaps
Morales et al. (2019)	Round et al. (1999), Li et al. (2018)	Witkowski & Lange-Bertalot (1993), Wetzel (2017, pers. comm.)	Li et al. (2018)	Witkowski et al. (2010)	Morales (2001), Beauger et al. (2018)

Associated flora: The new taxon was associated with *Nanofrustulum lucectorii* (11.9%, see above), *Amphora pediculus* (7.4%), *Pseudostaurosiropsis* sp. 2 (7.2%), *Nitzschia valdecostata* Lange-Bertalot & Simonsen (6.2%), *Karayevia clevei* (5.4%), and *Pseudostaurosiropsis* sp. 1 [5.4%, a form resembling *Pseudostaurosiropsis geocollegarum* (Witkowski) E.Morales].

The features presented for the two new taxa above and those included in Table 2 for species currently ascribed to *Nanofrustulum* put in evidence that the current description of this genus does not include the features present in many of these species.

Discussion

Both new species described herein belong to the genus *Nanofrustulum sensu* Round et al. (1999) and Morales et al. (2019) because both have the quasifract, fimbriate copulae, striae composed of areolae, interrupted by spines and they have apical pore fields.

Additionally, and following the emended description of the genus presented by Li et al. (2018), both taxa have a lanceolate sternum, alternating striae, serrate spines, and flaps present on the girdle areolae.

The detailed analysis of the morphology of all *Nanofrustulum* species presented in Table 2, shows that the emended description presented by Li et al. (2008) is in need of further expansion. This emended description does not account for the following characters: 1) cells are not only round to oval, but they can also be ovate as it happens in *N. rarissimum* E.Morales, Novais, C.E.Wetzel & Ector, *N. sourniae* (Chunlian Li, Riaux-Gobin & Witkowski) E.Morales, M.H.Novais & M.Morais, freshwater and marine representatives, respectively. 2) Striae are indeed uniseriate in the majority of species in the genus, but can also be biseriate as in *N. rarissimum*. 3) These striae are not always radiate about the axial area, but several taxa can also have parallel striae, especially in the middle of the valve, such is the case of the two new species presented herein, and every other taxon presented in Table 2, except *N. cataractarum*, which possesses striae entirely radiate. 4) Areolae on the valve mantle not only vary from 1–2, but more commonly 3 or 4 areolae are produced by different species or even up to 5 as in *N. cataractarum* and *N. squammatum* Riaux-Gobin & Witkowski, or even 6 areolae as in *N. sopotensis* (Witkowski & Lange-Bertalot) E.Morales, C.E.Wetzel & Ector and *N. trainorii* (E.Morales) E.Morales can be produced. 5) Areolae are not only round or transapically elongate, but also apically elliptic areolae can be found (the case of *N. sopotensis*), or a mixture of different shapes as is the case of *N. rarissimum* with round, square, or apically and transapically elongate areola; in the mantle these areolae are usually pervalvary elongate, squarish, rectangular, trapezoid or even elliptic following the different species. 6) Another feature is that of the margins of the spine tips, which are not only serrate, but can also be smooth as in *N. rarissimum*. 7) The stipules ("lateral projections" in the terminology of Li et al. 2018) can be present or absent as is the case in *N. cataractarum*, *N. krumbeinii* (A.Witkowski, Witak & K.Stachura) E.Morales, *N. rarissimum*, *N. sourniae* and *N. squammatum*. 8) In the case of apical pore fields, they can be present on one or two valve apices or can be absent, and can be composed by two or more pores of different disposition. 9) Finally, mantle plaques can indeed be present in the majority of species, but they can also be absent as in *N. lucectorii* sp. nov. and *N. squammatum*.

The emended description of *Nanofrustulum* presented herein is not restrictive to the characters described in Table 2, but rather leaves room for inclusion of other potentially new species that might be characterized by new character states or novel combinations of features.

Table 2 contains unique characters (in bold) for each of the species currently included in *Nanofrustulum*. The number of these unique features ranges from one (as for *N. trainorii*) to five (as for *N. cataractarum*). *Nanofrustulum lucectorii* is unique (Table 2) in that 1) its valves are elliptic in shape with broadly rounded apices; 2) its spines have a solid core with an apically elliptic base, with a flattened body and spatulate, serrate tips that are wider than the spine body; 3) the spines have rectangular stipules that cover the first subtending mantle areola; and 4) the apical pore fields, present at both valve ends, are similar in size and composed of a single transapical row of sunken pores.

Though there are overlaps at the lower side of the size range, the valves of *N. lucectorii* are among the largest among species in the genus, reaching up to 11.5 µm in length, being second only to *N. sourniae* (Table 2). Because of this large size, and the shape of the valves of the new species, the latter is identifiable under LM, under which the areolae are also clearly resolved.

Nanofrustulum ibericum is mainly defined by its 1) solid spines with a triangular of trapezoid base, and an also triangular and recurved body; and 2) the shape of the blisters on the abvalvar side of the mantle that are pervalvary rectangular and widely spaced, a feature not observed in any other species of the genus (Table 2). This new taxon is more difficult to distinguish from other taxa with valves having a shape that is broadly elliptic with broadly rounded apices, except perhaps because (for now) the new taxon is only reported from temporary ecosystems, the fact that perfectly round valves have not been found in type or any other material coming from these temporary ecosystems, and the observation that obtuse apices are seen in other taxa with broadly elliptic taxa, but never in the new species (Table 2).

Though, and as shown in the Introduction, there might be a debate regarding the classification of the Staurosiraceae, based on Table 1 in Morales et al. (2019), its seems that staurosiroid genera can be separated based on morphological distinguishing features, though such a table is preliminary to the establishment of diagnostic characters. Notwithstanding, the distinguishing feature of *Nanofrustulum* remains the quasifract bands.

Unfortunately, the information in published literature regarding the fine structure of girdle bands in all *Nanofrustulum* species is poor and needs to include further detailed studies. SEM or TEM images of these girdle elements are not clear altogether. For now, we can deduce that the valvocopula in some taxa is entire and open (as in *N. lucectorii*, see Fig. 29, valvocopula is denoted by asterisk), while in other taxa it can be quasifract (e.g. *N. cataractarum*, see Wetzel et al. 2013). Likewise, the shape (of the main body and the fimbriae) of quasifract girdle elements is variable at least for some taxa. For example, contrast the deeper and more robust elements with tongue-like fimbriae that can be positioned on the center or on the side of the main body of the element in *N. shiloi* (Li et al. 2018, figs. 294, 295) with the scaly, much smaller quasifract copulae with a faint central fimbria in *N. neoellipticum* (Witkowski) E.Morales (Morales 2021, fig. 15). Therefore, a closer study and consideration of the girdle band structure in species of *Nanofrustulum* might yield an additional set of characters to distinguish species.

Ecologically, *Nanofrustulum* can be found in marine, brackish and freshwater. This is also the case of other staurosiroid genera such as for instance *Pseudostaurosira* and *Pseudostaurosiropsis* of which both freshwater and brackish water representatives have been reported (Williams & Round 1988, Witkowski & Lange-Bertalot 1995, Seddon et al. 2014, Morales 2022). As wider geographical areas are studied and diatoms are analyzed by paired LM and SEM techniques, it becomes evident that genera thought to be restricted to a single type of habitat might encompass a wider number of species, spread over an also wider number of habitats (see the studies cited above). This consideration

should also permeate into applied studies as stated by Li et al. (2018), where researchers should refrain from fitting taxa into particular genera simply because a given genus is only known from a particular type of environment. We do also agree with Li et al. (2018) that for the identification and taxonomy of smaller forms such as "araphid" taxa lacking rimoportula, in general, or *Nanofrustulum* spp. in particular, the use of ultrastructural features is required for a proper identification at the species level, as it is shown in our Table 2.

The two new taxa described here are the first occurrences from temporary rivers, confirmed by LM and SEM observations. We reiterate the fact that some of these new species found in flowing waters, in stagnant pools, and more commonly in dry biofilms during the dry phase of these intermittent streams are key elements to the study of the ecology of these ecosystems, but also and because some of them can be more abundant and dominant in dry biofilm, they can be used in a continued biomonitoring of temporary systems throughout an entire year (as shown in Novais et al. 2020).

Acknowledgements

References

Anonymous (1975). Proposals for a standardization of diatom terminology and diagnoses. *Nova Hedwigia. Beiheft, 53*, 323–354.

A.P.A, I.P. (2016). *Plano de gestão de região hidrografica 2016/2021. Parte 2 – Caracterização e Diagnóstico*. Anexo IV. Agência Portuguesa do Ambiente, I.P.

Ashworth, M. P., Ruck, E., Lobban, C. S., Romanovicz, D. K., & Theriot, E. C. (2012). A revision of the genus *Cyclophora* and description of *Astrosyne* gen. nov. (Bacillariophyta), two genera with the pyrenoids contained within pseudosepta. *Phycologia, 51*(6), 684–699. https://doi.org/10.2216/12-004.1

Barber, H. G., & Haworth, E. Y. (1981). A Guide to the Morphology of the Diatom Frustule with a Key to the British Freshwater Genera. *Scientific Publication – Freshwater Biological Association, 44*, 1–112.

Beauger, A., Wetzel, C. E., Voldoire, O., & Ector, L. (2018). *Pseudostaurosira bardii* (Fragilariaceae, Bacillariophyta), a new species from a saline hydrothermal spring of the Massif Central (France). *Botany Letters, 166*, 1–11.

Cemagref (1982). *Etude des méthodes biologiques quantitatives d'appréciation de la qualité des eaux*. Rapport Division Qualité des Eaux Lyon. Agence financière de Bassin Rhône-Méditerranée-Corse, Pierre-Bénite, France.

Cox, E. J. (2010). Morphogenetic information and the selection of taxonomic characters for raphid diatom systematics. *Plant Ecology and Evolution, 143*(3), 271–277. https://doi.org/10.5091/plecevo.2010.403

Demirel, Z., Imamoglu, E., & Dalay, M. C. (2020). Growth kinetics of *Nanofrustulum shiloi* under different mixing conditions in flat-plate photobioreactor. *Brazilian Archives of Biology and Technology, 63*, e20190201. https://doi.org/10.1590/1678-4324-2020190201

Frankovich, T. A., Ashworth, M. P., Sullivan, M. J., Theriot, E. C., & Stacy, N. I. (2018). Epizoic and apochlorotic *Tursiocola species* (Bacillariophyta) from the skin of Florida manatees (*Trichechus manatus latirostris*). *Protist, 169*(4), 539–568. https://doi.org/10.1016/j.protis.2018.04.002

Glaviano, F., Ruocco, N., Somma, E., De Rosa, G., Campani, V., Ametrano, P., . . . Zupo, V. (2021). Two benthic diatoms, *Nanofrustulum shiloi* and *Striatella unipunctata*, encapsulated in alginate beads, influence the reproductive efficiency of *Paracentrotus lividus* by modulating the gene expression. *Marine Drugs, 19*(4), 230. https://doi.org/10.3390/md19040230

Glezer, S.I., Makarova, I.V., Moisseeva, A.I. & Nikolaev, V.A. (1992). *The diatoms of the USSR fossil and recent. Vol. II. fasc. 2: Stephanodiscaceae, Ectodictyonaceae, Paraliaceae, adialiplicataceae, Pseudopodosiraceae, Trochosiraceae, Melosiraceae, Aulacosiraceae.* Vol. 2, Fasc. 2. 26 pp., St. Petersburg: NAUKA St.-Petersburg branch.

Grana, L., Morales, E. A., Besta, T., Echazú, D., Wetzel, C. E., Novais, M. H., . . . Maidana, N. I. (2015). On the geographical distribution and ecology of *Pseudostaurosira cataractarum* (Bacillariophyceae): New findings in the Palearctic and Neotropical ecozones. *Revista Brasileira de Botânica. Brazilian Journal of Botany, 38*(4), 809–821. https://doi.org/10.1007/s40415-015-0188-0

Hofmann, G., Werum, M., & Lange-Bertalot, H. (2011). *Diatomeen im Süßwasser-Benthos von Mitteleuropa. Bestimmungsflora Kieselalgen für die ökologische Praxis. Über 700 der häufigsten Arten und ihre Ökologie*. Rugell: A.R.G. Gantner Verlag K.G.

INAG I.P. (2008). *Manual para a Avaliação Biológica da Qualidade da Agua em Sistemas Fluviais Segundo a Directiva-Quadro da Água – Protocolo de Amostragem e Análise para o Fitobentos – Diatomáceas*. – Ministério do Ambiente, do Ordenamento do Território e do Desenvolvimento Regional. Instituto da Água, I.P., Lisboa.

Krammer, K., Lange-Bertalot, H. (1986). Bacillariophyceae 1. Teil: Naviculaceae. In H. Ettl, J. Gerloff, H. Heynig, & D. Mollenhauer (Eds.), *Süsswasserflora von Mitteleuropa 2/1*, 1–876 pp. Gustav Fischer Verlag, Stuttgart, Jena.

Krammer, K., & Lange-Bertalot, H. (1988). Bacillariophyceae 2. Teil: Bacillariaceae, Epithemiaceae, Surirellaceae. In H. Ettl, J. Gerloff, H. Heynig, & D. Mollenhauer (Eds.), *Süsswasserflora von Mitteleuropa 2/2,* 1–596 pp. Stuttgart, Jena: Gustav Fischer Verlag.

Krammer, K., Lange-Bertalot, H. (1991a). Bacillariophyceae 3. Teil: Centrales, Fragilariaceae, Eunotiaceae. In H. Ettl, J. Gerloff, H. Heynig, & D. Mollenhauer (Eds.), *Süsswasserflora von Mitteleuropa 2/3*, 1–576 pp. Gustav Fischer Verlag, Stuttgart, Jena.

Krammer, K., & Lange-Bertalot, H. (1991b). Bacillariophyceae 4. Teil: Achnanthaceae. Kritische Ergänzungen zu *Navicula* (Lineolatae) und *Gomphonema*. Gesamtliteraturverzeichnis Teil 1–4.

In H. Ettl, J. Gerloff, H. Heynig, & D. Mollenhauer (Eds.), *Süsswasserflora von Mitteleuropa 2/4,* 1–437 pp. Stuttgart, Jena: Gustav Fischer Verlag.

Lange-Bertalot, H., & Genkal, S. I. (1999). Diatoms from Siberia I - Islands in the Arctic Ocean (Yugorsky-Shar Strait) Diatomeen aus Siberien. I. Insel im Arktischen Ozean (Yugorsky-Shar Strait). *Iconographia Diatomologica, 6,* 1–271.

Lange-Bertalot, H., Hofmann, G., Werum, M., & Cantonati, M. (2017). *Freshwater Benthic Diatoms of Central Europe: Over 800 Common Species Used in Ecological Assessment*. English Edition with Updated Taxonomy and Added Species (M. Cantonati, M. G. Kelly, & H. Lange-Bertalot, Eds.). Koeltz Botanical Books, Schmitten-Oberreifenberg.

Lecointe, C., Coste, M., & Prygiel, J. (1993). "Omnidia": Software for taxonomy, calculation of diatom indices and inventories management. *Hydrobiologia, 269-270*(1), 509–513. https://doi.org/10.1007/BF00028048

Lee, J. J., Reimer, C. W., & McEnery, M. E. (1980). The identification of diatoms isolated as endosymbionts from larger Foraminifera from the Gulf of Eilat (Red Sea) and the description of 2 new species, *Fragilaria shiloi* sp. nov. and *Navicula reissii* sp. nov. *Botanica Marina, 23*(1), 41–48. https://doi.org/10.1515/botm.1980.23.1.41

Li, C., Witkowski, A., Ashworth, M. P., Dabek, P., Sato, S., Zglobicka, I., . . . Kwon, Ch.-J. (2018). The morphology and molecular phylogenetics of some marine diatom taxa within the Fragilariaceae, including twenty undescribed species and their relationship to *Nanofrustulum, Opephora* and *Pseudostaurosira. Phytotaxa, 355*(1), 1–104. https://doi.org/10.11646/phytotaxa.355.1.1

Li, Y., Gao, Y-H. & Lü, S-L. (2008). *Nanofrustulum*, a new record of nanodiatom genus in China. *Journal of Systematics and Evolution, 46*, 750–753.

López-Fuerte, F. O., Lora-Vilchis, M. C., Veleva, L., Siqueiros-Beltrones, D. A., Arredondo-Vega, B. O., & Virgen-Felix, M. (2016). Primeros registros de *Nanofrustulum shiloi* (Lee, Reimer & McEnery) Round, Hallsteinsen & Paasche y *Nitzschia neinhusii* Sterrenburg & Sterrenburg (Bacillariophyceae, Ochrophyta) en aguas mexicanas. *CICIMAR Oceánides, 31*, 35–41. https://doi.org/10.37543/oceanides.v31i1.163

Medlin, L., & Desdevises, Y. (2016). Phylogeny of 'araphid' diatoms inferred from SSU and LSU rDNA, RBCL and PSBA sequences. *Vie et Milieu, 66*, 129–154.

Morales, E. A. (2001). Morphological studies in selected fragilarioid diatoms (Bacillariophyceae) from Conneticut waters (U.S.A.). *Proceedings. Academy of Natural Sciences of Philadelphia, 151*(1), 105–120. https://doi.org/10.1635/0097-3157(2001)151[0105:MSISFD]2.0.CO;2

Morales, E. A. (2021). Transfer of *Fragilaria neoelliptica* Witkowski to the genus *Nanofrustulum* Round, Hallsteinsen & Paasche (Fragilariaceae, Bacillariophyta). *Notulae Algarum, 205*, 1–4.

Morales, E. A. (2022). Two new species of *Pseudostaurosiropsis* (Bacillariophyta, Fragilariophyceae) from the United States of America, with taxonomic comments on the genus. *Algae – Korean Phycological Society, 37*, 33–47. https://doi.org/10.4490/algae.2022.37.11.15

Morales, E. A., Siver, P. A., & Trainor, F. R. (2001). Identification of (Bacillariophyceae) during ecological assessments: Comparison between Light Microscopy and Scanning Electron Microscopy techniques. *Proceedings. Academy of Natural Sciences of Philadelphia, 151*, 29–37. https://doi.org/10.1635/0097-3157(2001)151[0095:IODBDE]2.0.CO;2

Morales, E. A., Wetzel, C. E., & Ector, L. (2021). New and poorly known "araphid" diatom species (Bacillariophyta) from regions near Lake Titicaca, South America and a discussion on the continued use of morphological characters in "araphid" diatom taxonomy. *PhytoKeys, 187*, 23–70. https://doi.org/10.3897/phytokeys.187.73338

Novais, M. H., Hlúbiková, D., Morais, M., Hoffmann, L., & Ector, L. (2011). Morphology and ecology of *Achnanthidium caravelense* (Bacillariophyceae), a new species from Portuguese rivers. *Algological Studies, 136-137*, 131–150. https://doi.org/10.1127/1864-1318/2011/0136-0131

Novais, M. H., Morales, E. A., Penha, M. A., Potes, M., Bouchez, A., Barthès, A., . . . Morais, M. (2020). Benthic diatom community dynamics in Mediterranean intermittent streams: Effects of water availability and their potential as indicators of dry-phase ecological status. *The Science of the Total Environment, 719*, 137462. https://doi.org/10.1016/j.scitotenv.2020.137462

Patterson, C., Williams, D. M., & Humphries, C. J. (1993). Congruence between molecular and morphological phylogenies. *Annual Review of Ecology and Systematics, 24*(1), 153–188. https://doi.org/10.1146/annurev.es.24.110193.001101

Reichardt, E. (1997). Taxonomische Revision des Artenkomplexes um *Gomphonema pumilum* (Bacillariophyceae). *Nova Hedwigia, 65*, 99–129. https://doi.org/10.1127/nova.hedwigia/65/1997/99

Ross, R., Cox, E. J., Karayevia, N. I., Mann, D. G., Paddock, T. B. B., Simonsen, R., & Sims, P. A. (1979). An amended terminology for the siliceous components of the diatom cell. *Nova Hedwigia. Beiheft, 64*, 513–533.

Round, F. E., Crawford, R. M., & Mann, D. G. (1990). *The Diatoms: Biology & Morphology of the Genera*. Cambridge, U.S.A.: Cambridge University Press.

Round, F. E., Hallsteinsen, H., & Paasche, E. (1999). On a previously controversial "fragilarioid" diatom now placed in a new genus *Nanofrustulum. Diatom Research, 14*(2), 343–356. https://doi.org/10.1080/0269249X.1999.9705476

Ruocco, N., Costantini, S., Zupo, V., Lauritano, C., Caramiello, D., Ianora, A., . . . Costantini, M. (2018). Toxigenic effects of two benthic diatoms upon grazing activity of the sea urchin: Morphological, metabolomic and *de novo* transcriptomic analysis. *Scientific Reports, 8*(1), 5622. https://doi.org/10.1038/s41598-018-24023-9

Ruocco, N., Nuzzo, G., D'Ippolito, G., Manzo, E., Sardo, A., Ianora, A., . . . Fontana, A. (2020). Lipoxygenase pathways in diatoms: Occurrence and correlation with grazer toxicity in four benthic diatoms. *Marine Drugs, 18*(1), 66. https://doi.org/10.3390/md18010066

Sar, E., & Sunesen, I. (2003). *Nanofrustulum shiloi* (Bacillariophyceae) from the Gulf of San Matías (Argentina): Morphology, distribution and comments about nomenclature. *Nova Hedwigia, 77*(3-4), 399–406. https://doi.org/10.1127/0029-5035/2003/0077-0399

Seddon, A. W. R., Witkowski, A., Froyd, C. A., Kurzydlowski, K. J., Grzonka, J., & Willis, K. J. (2014). Diatoms from isolated islands II: *Pseudostaurosira diablarum*, a new species from a mangrove ecosystem in the Galápagos Islands. *Diatom Research, 29*(2), 201–211. https://doi.org/10.1080/0269249X.2013.877084

Theriot, E. C., Ashworth, M. P., Ruck, E., Nakov, T., & Jansen, R. K. (2010). A preliminary multigene phylogeny of the diatoms (Bacillariophyta): Challenges for future research. *Plant Ecology and Evolution, 143*(3), 278–296. https://doi.org/10.5091/plecevo.2010.418

Van de Vijver, B., Ector, L., Beltrami, M. E., de Haan, M., Falasco, E., Hlúbiková, D., . . . Wojtal, A. Z. (2011). A critical analysis of the type material of *Achnanthidium lineare* W. Sm. (Bacillariophyceae). *Algological Studies, 136-137*, 167–191. https://doi.org/10.1127/1864-1318/2011/0136-0167

Wetzel, C. E., Morales, E. A., Blanco, S., & Ector, L. (2013). *Pseudostaurosira cataractarum* comb. nov. (Bacillariophyta): Type analysis, ecology and world distribution of a former "centric" diatom. *Acta Nova, 6*, 53–63.

Williams, D. M. (2006). Some notes on the classification of *Fragilaria, Synedra* and their subgroups. *Nova Hedwigia. Beiheft, 130*, 17–34.

Williams, D. M. (2013). Why is *Synedra* berolinensis so hard to classify? More on monotypic taxa. *Phytotaxa, 127*(1), 113–127. https://doi.org/10.11646/phytotaxa.127.1.13

Williams, D. M., & Round, F. E. (1987). Revision of the genus *Fragilaria. Diatom Research, 2*(2), 267–288. https://doi.org/10.1080/0269249X.1987.9705004

Witkowski, A., & Lange-Bertalot, H. (1993). Established and new diatom taxa related to *Fragilaria schulzii* Brockmann. *Limnologica, 23*, 59–70.

Witkowski, A., Lange-Bertalot, H., & Witak, M. (1995). Diatom taxa of unusual frustule structure belonging to the genus *Fragilaria. Fragmenta Floristica et Geobotanica, 40*, 729–741.

Witkowski, A., Riaux-Gobin, C., & Daniszewska-Kowalczyk, G. (2010). New marine diatom littoral species (Bacillariophyta) from Kerguelen Islands. II. Heteropolar species of Fragilariaceae. *Vie et Milieu, 60*, 265–281.